

# The protein kinase M $\zeta$ network as a bistable switch to store neuronal memory

Hideaki Ogasawara<sup>1,2,§</sup> and Mitsuo Kawato<sup>2</sup>

<sup>1</sup>National Institute of Information and Communications Technology, 2-2-2,

Hikaridai, Seika, Kyoto 619-0288, Japan

<sup>2</sup>ATR Computational Neuroscience Laboratories, 2-2-2, Hikaridai, Seika,

Kyoto 619-0288, Japan

<sup>§</sup>Corresponding author

Email addresses:

HO: [ogahide.res@gmail.com](mailto:ogahide.res@gmail.com)

MK: [kawato@atr.jp](mailto:kawato@atr.jp)

## Abstract

### Background

Protein kinase M $\zeta$  (PKM $\zeta$ ), the brain-specific, atypical protein kinase C isoform, plays a key role in long-term maintenance of memory. This molecule is essential for long-term potentiation *in vitro* and various modalities of learning such as spatial memory and fear conditioning. It is not known, however, how PKM $\zeta$  stores information for long periods of time despite molecular turnover.

### Results

We hypothesized that PKM $\zeta$  forms a bistable switch because it appears to constitute a positive feedback loop (PKM $\zeta$  induces its local synthesis) part of which is ultrasensitive (PKM $\zeta$  stimulates its synthesis through dual pathways). To examine this hypothesis, we modeled the biochemical network of PKM $\zeta$  with realistic kinetic parameters. Bifurcation analyses of the model showed that the system maintains either the UP state or the DOWN state according to previous inputs. Furthermore, the model was able to reproduce a variety of previous experimental results regarding synaptic

plasticity and learning, which suggested that it captures the essential mechanism for neuronal memory. We proposed *in vitro* and *in vivo* experiments that would critically examine the validity of the model and illuminate the pivotal role of PKM $\zeta$  in synaptic plasticity and learning.

## Conclusions

This study revealed bistability of the PKM $\zeta$  network and supported its pivotal role in long-term storage of memory.

## Background

Protein kinase M $\zeta$  (PKM $\zeta$ ) is increasingly drawing attention as a molecule that maintains neuronal memory for an extremely long period of time [1]. It is a brain-specific atypical protein kinase C (PKC) isoform that lacks a regulatory domain, rendering it constitutively active [2]. PKM $\zeta$  enhances excitatory postsynaptic currents (EPSCs) and leads to the long-term potentiation (LTP) of synapses by stabilizing  $\alpha$ -amino-3-hydroxy-5-methyl-4-isoxazolepropionic acid (AMPA)-type

glutamate receptors through an N-ethylmaleimide-sensitive factor (NSF)/GluR2-dependent pathway [3-5]. The messenger ribonucleic acid (mRNA) for PKM $\zeta$  is found in various brain areas, including the hippocampus, striatum, neocortex, thalamic nuclei, and cerebellar cortex and localizes to spiny dendrites of neurons [6]. PKM $\zeta$  is translated within only ten minutes in response to LTP-inducing stimuli [2, 7], suggesting its local synthesis.

The use of a specific inhibitor,  $\zeta$ -inhibitory protein (ZIP) [8], has elucidated the pivotal role of PKM $\zeta$  in synaptic plasticity, learning, and memory. The late phase of LTP (L-LTP) in a hippocampal slice is reversed by ZIP administration [9], indicating that LTP maintenance requires PKM $\zeta$ . PKM $\zeta$  plays crucial roles in various modalities of learning, including spatial memory of the hippocampus and fear conditioning of the basal lateral amygdala, as evidenced by memory erasure following ZIP microinjection [10]. In rats, consolidated memory is sensitive to ZIP for at least one month [11].

PKM $\zeta$  appears to constitute a positive feedback loop [1, 12, 13]. ZIP administration prevents hippocampal neurons from expressing PKM $\zeta$  protein when these neurons are treated with a tetanus that would normally induce LTP and PKM $\zeta$  expression [12], indicating that PKM $\zeta$  activity is necessary for PKM $\zeta$  synthesis. We previously posed the possibility that the PKM $\zeta$  network is bistable [13], since biochemical positive feedback loops often offer bistability [14, 15]. Bistable positive feedback loops of enzymatic reactions may provide a basis for cellular memory [16, 17].

Our previous model [13, 18] conceptually illustrated that memory plasticity and stability can be both achieved by a cascade of multiple nonlinear or bistable dynamics that have various time constants and are connected in tandem in the order of fast to slow. Once the cascade is stimulated, activity is transmitted from a fast dynamic to a slower dynamic before the faster dynamic loses its activity; finally, the slowest dynamic is turned on.

Hippocampal LTP appears to occur in line with this model. LTP-inducing stimuli trigger a supralinear calcium increase in dendritic spines that lasts for seconds [19-22]. Then, calcium activates protein kinases such as  $\text{Ca}^{2+}$ /calmodulin-dependent protein kinase (CaMKII) in a supralinear manner and maintains their activity for tens of minutes [23, 24]. Finally, CaMKII and other protein kinases induce longer-lasting PKM $\zeta$  expression [12] in an all-or-none manner [13].

To evaluate our hypothesis that the PKM $\zeta$  network is bistable and functions as neuronal memory, we performed simulations and bifurcation analyses in the Results section. Our model was able to reproduce the results of a variety of previous experiments. Moreover, in the Discussion section, we proposed experiments that would critically examine our hypothesis in the Discussion section. Although ZIP is regarded as a specific inhibitor of PKM $\zeta$ , it might inhibit other protein kinases as well. In this paper, therefore, we use the term ‘PKM $\zeta$ ’ to collectively refer to ZIP-sensitive protein kinases including

PKM $\zeta$ .

## Results

### Description of the model

Figure 1 illustrates the molecular pathways of the PKM $\zeta$  network model.

The model is described by three ordinary differential equations (ODEs),

Equations 1-3 (see Materials and Methods for details). A time-dependent

variable, Stim(t), represents the aggregate activity of protein kinases,

including CaMKII, PKC, and MAPK, which triggers PKM $\zeta$  expression

(Figure 1, arrow 1) [2, 7]. In reality, these protein kinases act through

various pathways to turn on the PKM $\zeta$  network. However, since the purpose

of the model was to mathematically analyze the dynamics of the network,

kinasic activation of the network was simplified as a single variable.

Experiments have shown that the PKM $\zeta$  protein stimulates translation of

its own mRNA into protein (Figure 1 arrow 2) [25], forming a positive

feedback loop. At the same time, its PKC activity promotes actin

polymerization (Figure 1 arrow 3) [26-29], and F-actin (actin polymer)

facilitates general protein synthesis (Figure 1 arrow 4) [30, 31]. This convergence of the two pathways may make the system more sensitive to differences in stimulus size than the standard Michaelis-Menten kinetics (ultrasensitivity). A mathematical theory states that a combination of ultrasensitivity and positive feedback possibly results in bistability [15], which we examine in the following section.

#### Bistability of the PKM $\zeta$ network

We stimulated the model with a square wave,  $\text{Stim}(t) = 5, 25$  or  $125$  ( $0 \leq t < 30$ ), to observe the time course of [PKM $\zeta$ ] (Figure 2A). EPSC amplitudes (Figure 2B) were estimated by time-integrating [PKM $\zeta$ ] (Equation 4 in Materials and Methods). In this model, the concentrations of molecules and strength of Stim are unitless values, and EPSC amplitudes of 1 and 2 correspond to the unpotentiated and potentiated states, respectively. When the stimulus was weak (Stim = 5), [PKM $\zeta$ ] rose transiently but ended up at zero, and EPSC was enhanced transiently. When the stimulus was intermediate (Stim = 25), [PKM $\zeta$ ] reached a value of 0.72 asymptotically,

and EPSC amplitude reached a value of 2. When the stimulus was strong (Stim = 125),  $[\text{PKM}\zeta]$  overshoot before asymptotically reaching a value of 0.72, and EPSC amplitude approached a value of 2 asymptotically. The response appeared to be a switch because strong and intermediate stimuli resulted in the same steady state, whereas weak stimuli resulted in a distinct steady state.

We then varied the duration and strength of Stim(t) to see whether  $[\text{PKM}\zeta]$  can reach any steady state other than  $[\text{PKM}\zeta]_{t=\infty} = 0$  or 0.72. In the two-dimensional parameter space (Figure 3A) with respect to the strength (abscissa) and duration (ordinate),  $[\text{PKM}\zeta]_{t=\infty}$  was either 0 (gray) or 0.72 (white), and not intermediate anywhere. Stimuli that were longer or shorter in duration required a weaker or stronger strength, respectively, to turn on the PKM $\zeta$  network. As expected, EPSC amplitude reached a value of either 1 or 2 (Figure 3B), and the areas for EPSC  $_{t=\infty} = 1$  and EPSC  $_{t=\infty} = 2$  were identical to the areas for  $[\text{PKM}\zeta]_{t=\infty} = 0$  and  $[\text{PKM}\zeta]_{t=\infty} = 0.72$ , respectively.

This switch-like behavior indicates high nonlinearity of the system.

Up to this point, we have shown that the PKM $\zeta$  network responds to stimuli in an all-or-nothing manner (Figures 2 and 3). Next, we performed a bifurcation analysis [32-34] to further illuminate the dynamics of the model and evaluate its parameter dependence. The model has seven parameters, including the rate parameters  $j_1$ ,  $j_2$ ,  $j_3$ , and  $j_4$  and three time constants (see Materials and Methods), but we only needed to analyze the model with respect to the four rate parameters because the time constants do not affect the model equilibria (see additional file 1).  $j_1$  denotes the PKM $\zeta$  synthesis rate relative to its decay rate,  $j_2$  and  $j_3$  denote the PKM $\zeta$ -independent and PKM $\zeta$ -dependent actin polymerization rates relative to the actin depolymerization rate, respectively, and  $j_4$  denotes the rate at which PKM $\zeta$  mRNA is incorporated into the translational machinery relative to the rate of mRNA detachment from the machinery.

First, we varied the PKM $\zeta$  synthesis rate  $j_1$  and tracked the equilibrium points of the model (Figure 4A). The horizontal and vertical axes show  $j_1$  and steady-state [PKM $\zeta$ ], respectively. The two solid lines denote stable steady states: the UP state (upper) and the DOWN state (lower). There are two saddle-node bifurcations (circles) at  $j_1 = 53$  and  $j_1 = 100$ . When  $j_1 < 53$ , only the DOWN state is stable; when  $j_1 > 100$ , only the UP state is stable. When  $53 \leq j_1 \leq 100$ , the system is bistable at the two stable steady states, the UP and DOWN states, which are separated by an unstable steady state (dashed line). The default value of  $j_1$  is 80 and is within the range of bistability.

Next, we performed a bifurcation analysis with respect to the PKM $\zeta$ -independent actin polymerization rate  $j_2$  and the PKM $\zeta$ -dependent polymerization rate  $j_3$ . Figure 4B shows  $j_2$  on the horizontal axis and steady-state [PKM $\zeta$ ] on the vertical axis. There is a saddle-node bifurcation (SN1) at  $j_2 = 0.066$ , and the system is bistable when  $j_2 < 0.066$  and

monostable at the UP state when  $j_2 \geq 0.066$ . To further characterize the actin polymerization rates-dependent dynamics of the model, we performed two-parameter bifurcation analysis with respect to  $j_2$  and  $j_3$  (Figures 4C and 4D). The analysis revealed that two branches of the saddle node bifurcation curve (solid lines, SN1 and SN2) meet tangentially at a point (solid circle). This type of bifurcation is mathematically termed the "cusp bifurcation" [34]. The parameter regions of monostability and bistability are indicated in Figure 4C. Loss of bistability at small values of  $j_2$  and  $j_3$  indicates that the F-actin-dependent facilitation of protein synthesis is essential for the bistability of the PKM $\zeta$  network.

Lastly, we performed a bifurcation analysis in terms of  $j_4$ , the rate at which PKM $\zeta$  mRNA is incorporated into the translational machinery (Figure 4E). The system is monostable at the DOWN state when  $j_4 < 0.10$  or at the UP state when  $j_4 > 0.19$ . It is bistable when  $0.10 \leq j_4 \leq 0.19$ .

The PKM $\zeta$  network was shown to be bistable over wide ranges of the parameters  $j_1$ ,  $j_2$ ,  $j_3$ , and  $j_4$ , indicating the robustness of the bistability of the model.

### Comparison with previous experiments

We demonstrated that the PKM $\zeta$  network is robustly bistable and thus capable of storing information. Next, we simulated a variety of previous experiments to examine whether the model was able to explain their results.

ZIP reverses LTP even when applied as much as five hours after LTP-inducing stimuli [9], indicating the essential role of PKM $\zeta$  in L-LTP.

We simulated this experiment by starting from the UP state and temporarily clamping [PKM $\zeta$ ] at zero for 60 min. The simulated time courses of [PKM $\zeta$ ] and EPSC amplitude are plotted in Figures 5A and 5B.

When PKM $\zeta$  was eliminated, EPSC amplitude began to gradually decrease.

When [PKM $\zeta$ ] was unclamped at  $t = 60$ , it increased slightly, hit a peak, and decreased again, whereas EPSC amplitude constantly approached the

DOWN state. Thus, the simulation result is consistent with the previous experimental result [9].

The introduction of exogenous PKM $\zeta$  is sufficient to induce LTP in CA1 pyramidal neurons [25]. We simulated this experiment by fixing [PKM $\zeta$ ] at 10 for 5 min to mimic exogenous PKM $\zeta$ . The simulated time courses of endogenous [PKM $\zeta$ ] and EPSC amplitude are shown in Figures 5C and 5D.

Similar to the experimental result, transient application of exogenous PKM $\zeta$  activated PKM $\zeta$  production and turned on the positive feedback loop, which perpetually maintained endogenous PKM $\zeta$  expression and enhanced EPSC amplitude.

Injection of protein synthesis inhibitor does not erode the consolidated memory of a behaving animal unless the memory is recalled simultaneously with the injection [35-37]. We simulated the inhibition of protein synthesis in a potentiated synapse by setting  $j_l$  to 0 during  $0 \leq t < 540$ . The duration

of inhibition was based on a report that microinfusion of anisomycin into the hippocampus inhibited protein synthesis for 9 h [38]. The simulated time courses of [PKM $\zeta$ ] and EPSC amplitude are plotted in Figures 5E and 5F. PKM $\zeta$  was degraded so slowly that only a small portion was lost while  $j_1 = 0$  for 540 min, and the level returned to that of the UP state value when  $j_1$  was recovered. This result is consistent with the fact that transient protein synthesis inhibition does not usually affect consolidated memory [35-37].

Actin assembly inhibitors such as cytochalasins and latrunculins inhibit LTP induction [39]. We simulated the temporal application of an actin assembly inhibitor by setting  $j_2$  and  $j_3$  to 0 for 60 min. The simulated time courses are plotted in Figures 5G and 5H. In agreement with experimental results, a stimulus that would have activated the PKM $\zeta$  positive feedback loop in the control condition failed to do so when actin assembly was inhibited temporarily.

## Reconsolidation

Upon retrieval, well-consolidated memories become labile and vulnerable to protein synthesis inhibitors (reactivation) before they are reconsolidated

[35-37]. Reactivation is thought to trigger a consolidation-like process

because reactivated memory and newly acquired memory have similar time

courses of susceptibility to protein synthesis inhibition: they are intact in

the short term but impaired in the long term when a protein synthesis

inhibitor is administered either upon retrieval or upon *de novo* learning [40].

A reconsolidation-like process is also observable in slice electrophysiology

[41]; synapses that are potentiated by tetanus stimulation are depotentiated

when stimulated again in the presence of a protein synthesis inhibitor.

These findings indicate that carrier proteins of memory traces are depleted

on retrieval and replaced by newly synthesized proteins to restore memory,

as suggested previously [42]. Because PKM $\zeta$  is a carrier of long-term

memory, we, as well as other researchers, assumed an active mechanism

that destroys PKM $\zeta$  and induces its synthesis upon retrieval [1, 13, 37]. To

examine whether this assumption is consistent with previous experimental results, we simulated the time courses of [PKM $\zeta$ ] and EPSC amplitude after reactivation (Figures 5I and 5J). [PKM $\zeta$ ] was kept at zero during  $0 \leq t \leq 10$  to mimic reactivation, which we supposed would destroy PKM $\zeta$  proteins, and  $j_I$  was set at 0 when  $0 \leq t < 540$  and at the default value otherwise to mimic transient inhibition of protein synthesis. When the synapse was reactivated by a stimulus in the presence of a protein synthesis inhibitor, EPSC amplitude approached the DOWN state, and [PKM $\zeta$ ] did not recover after treatment. By contrast, [PKM $\zeta$ ] decreased transiently and subsequently recovered, ending up in the UP state, when the synapse was treated with either a reactivating stimulus or a protein synthesis inhibitor alone. These simulated results are in line with the process of reconsolidation seen in animal and slice experiments [35-37, 41]. However, the consistency between the simulation results and experimental data does not necessarily prove our hypothesis that newly synthesized PKM $\zeta$  replaces old PKM $\zeta$  upon

reactivation. Reconsolidation might also be explained by other plausible mechanisms.

## Discussion

Our model was extremely simple and lacked many of known pathways. Nevertheless, the model reproduced a variety of previous experimental results, suggesting that it captures the key characteristics of the PKM $\zeta$  network. In this section, we go a step further and propose future experiments to examine the validity of the model.

## Reconsolidation

We assume that in the neuron, a cascade of multiple nonlinear dynamics with various time constants are connected in tandem to store information stably and flexibly [13, 18]. According to this model, memory reactivation switches off the slowest dynamic, the PKM $\zeta$  network and switches on

upstream dynamics (i.e., calcium increases and activates multiple protein kinases). We demonstrated the consistency between the simulation results and previous experiments to underpin our hypothesis that upon memory reactivation, newly synthesized PKM $\zeta$  replaces preexisting PKM $\zeta$  (Figures 5I and 5J). It is possible to take advantage of LTP reconsolidation *in vitro* (see Results section) [41] and verify this hypothesis. To examine whether PKM $\zeta$  is degraded upon reactivation, hippocampal neurons are first treated with labeled amino acids, and then LTP is induced. Several hours later when LTP is consolidated, the neurons are either reactivated by another tetanus or left unstimulated (control) in the absence of labeled amino acids. According to our assumption of reactivation-triggered degradation, the amount of labeled PKM $\zeta$  will rapidly decrease in reactivated neurons whereas it will remain constant in control neurons. To prove synthesis of PKM $\zeta$  upon reactivation, LTP is first induced in hippocampal neurons in the absence of labeled amino acids. Several hours later, the neurons are either reactivated or left unstimulated (control) in the presence of labeled amino

acids. Our hypothesis predicts that reactivated neurons will synthesize a greater amount of labeled PKM $\zeta$  than control neurons, in which PKM $\zeta$  is produced only to meet its turnover.

It might also be possible to examine our hypothesis by *in vivo* experiments; hippocampal LTP is induced in behaving animals by inhibitory avoidance learning, in which animals are trained to associate the dark side of an experimental chamber with foot shocks [43]. First, the mouse PKM $\zeta$  gene is replaced with a PKM $\zeta$ -GFP chimeric gene. Then, the engineered mice are trained for an inhibitory avoidance task. Several days later, the preexisting PKM $\zeta$ -GFP in the hippocampus is photobleached, and the mice are divided into three groups: the reactivation group, the reactivation-protein synthesis inhibitor group, and the control group. The reactivation group mice are exposed to the experimental chamber to reactivate the fear memory. Those in the reactivation-protein synthesis inhibitor group are first administered a protein synthesis inhibitor and then exposed to the experimental chamber.

Control mice are exposed to another chamber distinct from the one used in the training sessions. It will be possible to quantify the newly synthesized PKM $\zeta$ -GFP by using fluorescence microscopy and the total PKM $\zeta$ -GFP (synthesized either before or after photobleaching) by an immunological methods.

Based on our hypothesis, a series of predictions can be made. In the reactivation group, PKM $\zeta$ -GFP fluorescence will increase, whereas the total amount of PKM $\zeta$ -GFP will remain constant. In the reactivation-protein synthesis inhibitor group, both the fluorescence and total amount of the chimeric protein will decrease. In the control group, the fluorescence will keep at a low level, and the total amount of PKM $\zeta$ -GFP will remain constant.

#### F-actin stabilizer

An F-actin stabilizer such as phalloidin [44] increases the ratio of the actin polymerization rate to the actin depolymerization rate. To predict the effect

of a F-actin stabilizer on the early phase of LTP, we omitted the decay term temporarily ( $0 \leq t \leq 60$ ) from the ODE for F-actin and simulated the time courses of [PKM $\zeta$ ] (Figure 6A) and EPSC amplitude (Figure 6B). In the presence of the F-actin stabilizer, the system resulted in the UP state when treated with a weak stimulus that would be insufficient to permanently activate the network in the control condition.

Next, we investigated how the F-actin stabilizer changes the dynamics of the model. A bifurcation diagram with respect to actin stability (Figure 6C) was obtained by slicing the two-parameter ( $j_2$  and  $j_3$ ) bifurcation plot (Figure 4D) with a perpendicular plane  $j_3 = aj_2$ , where “a” is a positive constant. The horizontal and vertical axes of the slice show  $j_2$  and the steady state [PKM $\zeta$ ], respectively. Solid circles indicate saddle-node bifurcations.  $j_2$  divided the dynamics of the model into three phases. The system was bistable when  $j_2$  was between 0.031 and 0.063 and monostable when  $j_2$  was outside of this range. A small rightward shift of  $j_2$  from the default value did not change

[PKM $\zeta$ ] significantly, but a large shift that crossed the right bifurcation point thrust the system into the UP state (arrow 1). Subsequent withdrawal of the F-actin stabilizer did not restore the DOWN state (arrow 2) and showed hysteresis, a characteristic feature of bistable systems. These simulations predicts that an F-actin stabilizer lowers the threshold of stimulation for LTP induction at low doses and induces LTP without stimuli at higher doses.

#### Variation of mRNA concentration

In recent years, remarkable *in vivo* techniques for gene transfer and local gene knockdown in the brain have been developed [45, 46]. In our model, we assumed a constant level of PKM $\zeta$  mRNA, but such methods will enable variation of [PKM $\zeta$  mRNA]. We predicted its outcome by performing a bifurcation analysis with respect to [PKM $\zeta$  mRNA] (default value of 1) as a bifurcation parameter (Figure 6D). The dynamics of the PKM $\zeta$  network was shown to be determined by [PKM $\zeta$  mRNA] and have three distinct phases. The system was monostable at the DOWN state when [PKM $\zeta$  mRNA] < 0.67

and at the UP state when  $[\text{PKM}\zeta \text{ mRNA}] > 1.2$ . The system was bistable when  $0.67 \leq [\text{PKM}\zeta \text{ mRNA}] \leq 1.2$ .

As  $[\text{PKM}\zeta \text{ mRNA}]$  increased, the saddle point approached the DOWN state (Figure 6D). One may assume that when the saddle point is closer to the DOWN state, the Stim threshold for switching on the system will be lower. Unfortunately, however, that assumption is not obvious from a two-dimensional projection (Figure 6D) of a system with many more dimensions. To obtain a clear view, we varied  $[\text{PKM}\zeta \text{ mRNA}]$  and found the Stim threshold (a square wave lasting for 30 min) necessary for turning the system on. Figure 6E plots the threshold value of Stim against  $[\text{PKM}\zeta \text{ mRNA}]$ . As predicted, the concentration and input threshold were negatively correlated. It would be possible to verify this prediction *in vitro* and *in vivo* by introducing a PKM $\zeta$  gene construct into the hippocampus. Moderate PKM $\zeta$  overexpression will lower the threshold for LTP induction and alter learning efficacy by increasing the sensitivity of the PKM $\zeta$

network to input, whereas an overdose of the gene will induce LTP without stimuli and hinder learning ability by destroying the bistability of the system. Silencing PKM $\zeta$  expression by RNA interference will also destroy the bistability of the system and prevent LTP and learning.

### Bistable positive feedback loop models

Bistable networks are ubiquitous in biology and are able to store information indefinitely despite the fact that individual molecules in the network turn over [16, 17]. Among the biological mechanisms for creating bistability, combinations of positive feedback and nonlinearity have been studied extensively. The MAPK positive feedback loop makes a bistable switch and plays crucial roles in development and memory [14, 47, 48]. Theoretical studies have shown that nonlinearity of the pathway arises from dual phosphorylations of the MAPK cascade; MAPK kinase kinase dually phosphorylates and activates MAPK kinase, and dually-phosphorylated MAPK kinase then dually phosphorylates MAPK [14, 49]. CaMKII is another example. It provides positive feedback by autophosphorylation.

According to a simulation study, the activity of CaMKII holoenzymes is bistable because the rate of autophosphorylation is nonlinearly dependent on the number of phosphorylated subunits [50]. In contrast to the MAPK and CaMKII models, our PKM $\zeta$  model is unique in that bistability arises in a positive feedback loop where two pathways activated by PKM $\zeta$  converge downstream and induce PKM $\zeta$  expression; this convergence was shown to be essential for bistability (Figure 4C). Similar translational switches in neuronal memory have been proposed recently. Aslam et al. modeled a bistable positive feedback loop consisting of CaMKII and a translational regulator, where CaMKII autophosphorylation activates translation of CaMKII [51].

#### Cerebellar long-term depression

Long-term depression of the parallel fiber-Purkinje cell synapse is thought to be the cellular substrate of cerebellar learning [52]. Cerebellar LTD shows remarkable similarity to hippocampal LTP, although they have different directions of plasticity and involve different receptor subunits; both

require large calcium transients and subsequent activation of CaMKII and PKC, and both follow AMPAR phosphorylation [52-56]. In the cerebellar Purkinje cell, stimuli induce a supralinear calcium influx, which activates MAPK and PKC in an all-or-none manner [48, 57-60]. MAPK and PKC are engaged in cerebellar LTD only in the early phase (approximately 30 min) [48, 60], and what maintains LTD in the later phase is not yet known. PKM $\zeta$ , the long-term memory trace in a variety of brain regions [1, 61], is also found in the cerebellar cortex [61], suggesting its potential involvement in cerebellar LTD [13, 18, 62]. This study mainly focuses on hippocampal L-LTP, but considering the similarity, it might also explain the mechanism for cerebellar memory.

## Conclusions

We have shown here that the PKM $\zeta$  network is robustly bistable, supporting its pivotal role in long-term memory. Obviously, PKM $\zeta$  is not the sole mechanism for long-term memory; expression of various proteins,

morphological changes, and synaptogenesis are also very important [63-69].

Interaction of molecular pathways that have different time scales is also important for memory stability [70]. Further experimental and computational studies will be necessary to address how these processes interact and cooperate and which process is the most crucial in retaining memory.

## Materials and Methods

### Simulation of the biochemical reactions

Figure 1 illustrates the pathways of the PKM $\zeta$  network model. Because qualitative data were not available for any of the pathways, we presumed the simplest case where each reaction was a first-order reaction. The following set of reactions describes the molecular interactions of the PKM $\zeta$  network. PKM $\zeta$  protein stimulates translation of its own mRNA (Figure 1 arrow 2) [25] and promotes actin polymerization (Figure 1 arrow 3) [26-29]. F-actin facilitates PKM $\zeta$ -induced PKM $\zeta$  synthesis (arrow 4) [31]. Stim(t) represents the collective activity of protein kinases, including PKC, MAPK,

and CaMKII, that induce PKM $\zeta$  expression (arrow 1) [2, 7, 12]; its basal value was 0.003, representing the background activity of the protein kinases.

The three ODEs that describe the reactions are as follows:

$$\tau_1 \frac{d[PKM\zeta]}{dt} = j_1[RNA_{active}](1 - [PKM\zeta]) - [PKM\zeta] \quad (1)$$

$$\tau_2 \frac{d[FActin]}{dt} = (j_2 + j_3[PKM\zeta])(1 - [FActin]) - [FActin] \quad (2)$$

$$\tau_3 \frac{d[RNA_{active}]}{dt} = j_4[FActin]([PKM\zeta] + Stim(t))(1 - [RNA_{active}]) - [RNA_{active}] \quad (3),$$

where  $[PKM\zeta]$ ,  $[FActin]$ , and  $[RNA_{active}]$  denote the concentrations of PKM $\zeta$  protein, actin protein molecules assembled into F-actin, and PKM $\zeta$  mRNA recruited into the local translational machinery ('active'), respectively.

In the model, concentrations are unitless quantities. In the future, when quantitative data are available, it would be simple to convert them into quantities with units (such as micromolar). Concentrations of total actin, including F-actin and G-actin (actin monomer), and total PKM $\zeta$  mRNA

(mRNA in and out of the translational machinery) are both assumed to be constant and designated values of one since neither actin or PKM $\zeta$  mRNA has been shown to increase or decrease upon LTP induction. Assuming biological regulation and resource limitation, the upper limit of [PKM $\zeta$ ] was set to one. The system was still bistable without this constraint (data not shown). Time has a unit of minutes. The time constants  $\tau_1$ ,  $\tau_2$ , and  $\tau_3$  were determined so that PKM $\zeta$  turnover, actin polymerization, and protein synthesis would take place in realistic time scales. The parameters  $j_1$ ,  $j_2$ ,  $j_3$ , and  $j_4$  denote reaction rates relative to the exponential decay of each variable:  $j_1$  designates the PKM $\zeta$  synthesis rate,  $j_2$  and  $j_3$  denote the PKM $\zeta$ -independent and PKM $\zeta$ -dependent actin polymerization rates, respectively, and  $j_4$  is the rate at which PKM $\zeta$  mRNA is incorporated into the translational machinery.

Equation 1 describes the processes in which PKM $\zeta$  is translated from its active mRNA and is degraded (Figure 1 arrow 1). The production rate has a

time scale of 10 min (depending on  $[RNA_{active}]$ ), which is comparable to experimental results [2]. Protein degradation was assumed to have a time scale of one day because the catalytic domain of PKC $\zeta$ , whose amino acid sequence is identical to that of full-length PKM $\zeta$ , is stable and has a half-life of at least one day [71]. Equation 2 refers to the reactions in which G-actin is transformed to F-actin and vice versa. The forward step is at least partly dependent on PKC $\zeta$  activity (Figure 1 arrow 3) [26-29]. Actin turnover in the dendritic spine was assumed to have a time scale of tens of seconds, based on previous experiments [72, 73]. Equation 3 describes the process in which PKM $\zeta$  mRNA is recruited into translation machinery in a  $[PKM\zeta]$ - and  $[FActin]$ -dependent manner (Figure 1 arrows 2, 3) [25].

PKM $\zeta$  enhances EPSC by stabilizing AMPA receptors in postsynaptic sites through an NSF/GluR2-dependent pathway [3-5]. AMPA receptors are composed of four subunits, including two GluR2s and two others [74, 75], and NSF is thought to interact with each GluR2 subunit [76]. Therefore, we

presumed that PKM $\zeta$ -dependent EPSC changes were a second-order reaction. EPSC was estimated by solving the following ODE:

$$\tau_4 \frac{d\text{EPSC}}{dt} = j_5(\text{EPSC}_{\text{UP}} - \text{EPSC}) \frac{[\text{PKM}\zeta]^2}{[\text{PKM}\zeta]_{\text{UP}}^2} - \text{EPSC} + j_6 \quad (4)$$

EPSC has an amplitude of 1 (arbitrary unit) in the DOWN state and an amplitude of 2 in the UP state ( $\text{EPSC}_{\text{UP}}$ ). ZIP application to potentiated hippocampal slices reduces the EPSC to the baseline level [9, 25], indicating that without PKM $\zeta$  activity, an augmented EPSC decays spontaneously. The time constant  $\tau_4$  was derived from previous experiments [9, 25].  $j_5$  was set to meet the initial rate of EPSC increase after postsynaptic introduction of exogenous PKM $\zeta$  [9, 25].  $j_6$  determines the basal level of EPSC.

Default parameters were represented by the following values:  $\tau_1 = 1500$ ,  $\tau_2 = 0.5$ ,  $\tau_3 = 60$ ,  $\tau_4 = 100$ ,  $j_1 = 80$ ,  $j_2 = 0.05$ ,  $j_3 = 0.5$ ,  $j_4 = 0.16$ ,  $j_5 = 14$ , and  $j_6 = 0.89$ .

We implemented the model equations into the software package XPPAUT [32] and performed numerical integrations and bifurcation analyses.

## Authors' contributions

HO designed and performed the study and drafted the manuscript. MK participated in the design the study and helped to draft the manuscript.

## Acknowledgements

We would like to thank Professor Nicolas Schweighofer of University of Southern California for helpful comments. This work was supported by a Grant-in-Aid for Scientific Research (KAKENHI 21700426).

## Figure legends

Figure 1. The PKM $\zeta$  network model. See text for explanation.

Figure 2. Time courses of A) [PKM $\zeta$ ] and B) EPSC amplitude. A weak (Stim = 5, solid line), intermediate (Stim = 25, dashed line) or strong (Stim = 125, dotted line) stimulus was given for 30 min. Stimulus strength, [PKM $\zeta$ ], and EPSC amplitude are unitless values.

Figure 3. Steady-state A)  $[\text{PKM}\zeta]$  and B) EPSC amplitude after various strengths and durations of Stim were given. The strength and duration of Stim are shown on the abscissa and the ordinate, respectively.

Figure 4. Bifurcation analyses. A) Bifurcation diagram with respect to the **PKM $\zeta$  synthesis rate,  $j_1$** . B) Bifurcation analysis with respect to the **PKM $\zeta$ -independent actin polymerization rate,  $j_2$** . Only one (SN1) of the two saddle node bifurcations is seen in this plot. C, D) Two-parameter bifurcation analysis with respect to  $j_2$ , and the **PKM $\zeta$ -dependent actin polymerization rate,  $j_3$** . C) A two-dimensional plot with  $j_2$  in the X-axis and  $j_3$  in the Y-axis. D) A three-dimensional plot with  $j_2$  in the X-axis,  $j_3$  in the Y-axis, and steady-state  $[\text{PKM}\zeta]$  in the Z-axis (log scale). E) Bifurcation analysis with respect to  $j_4$ , the rate at which **PKM $\zeta$  mRNA is incorporated into the translational machinery**. In panels A, B, and E, the solid and dashed lines indicate  $[\text{PKM}\zeta]$  at stable and unstable steady states,

respectively; the circles denote saddle-node bifurcations. In panels C and D, the solid lines, solid circles, and open circle (only in panel C) indicate saddle-node bifurcations (SN1 and SN2), the cusp bifurcation point, and the default values of  $j_1$  and  $j_2$ , respectively.

Figure 5. Simulations reproducing previous experimental results. Time courses of [PKM $\zeta$ ] (panels A, C, E, G, I) and EPSC amplitude (panels B, D, F, H, J) are shown. A, B) ZIP administration to a potentiated synapse. C, D) PKM $\zeta$  perfusion. E, F) Protein synthesis inhibitor administration to a potentiated synapse. G, H) A stimulus in the presence (solid line) or absence (dashed line) of an actin assembly inhibitor. I, J) Reactivation in the presence (solid line) or absence (dashed line) of protein synthesis inhibitor. The dotted line corresponds to administration of protein synthesis inhibitor without reactivation. Arrows and bold bars indicate the onset of an LTP-inducing stimulus,  $\text{Stim}(t) = 25$  ( $0 \leq t < 30$ ), and the duration of drug administration, respectively.

Figure 6. Simulations predicting experimental results. Time courses of A) [PKM $\zeta$ ] and B) EPSC amplitude after a weak stimulus,  $\text{Stim}(t) = 5$  ( $0 \leq t < 30$ ), in the presence (solid line) or absence (dashed line) of a F-actin stabilizer. C) Steady-state [PKM $\zeta$ ] versus an actin polymerization rate,  $j_2$ . The other actin polymerization rate,  $j_3$ , was treated as a dependent parameter ( $j_3 = 10j_2$ ). D, E) [PKM $\zeta$  mRNA] and bistability. D) Steady-state [PKM $\zeta$ ] versus the bifurcation parameter, [PKM $\zeta$  mRNA]. E) The threshold [PKM $\zeta$  mRNA] to perpetually activate the system.

## References

1. Sacktor TC: **PKM $\zeta$ , LTP maintenance, and the dynamic molecular biology of memory storage.** *Prog Brain Res* 2008, **169**:27-40.
2. Sacktor TC, Osten P, Valsamis H, Jiang X, Naik MU, Sublette E: **Persistent activation of the  $\zeta$  isoform of protein kinase C in the maintenance of long-term potentiation.** *Proc Natl Acad Sci USA* 1993, **90**:8342-8346.
3. Ling DS, Benardo LS, Sacktor TC: **Protein kinase M $\zeta$  enhances excitatory synaptic transmission by increasing the number**

- of active postsynaptic AMPA receptors. *Hippocampus* 2006, **16**:443-452.
4. Yao Y, Kelly MT, Sajikumar S, Serrano P, Tian D, Bergold PJ, Frey JU, Sacktor TC: **PKM $\zeta$  maintains late long-term potentiation by N-ethylmaleimide-sensitive factor/GluR2-dependent trafficking of postsynaptic AMPA receptors.** *J Neurosci* 2008, **28**:7820-7827.
  5. Miguez PV, Hardt O, Wu DC, Gamache K, Sacktor TC, Wang YT, Nader K: **PKM $\zeta$  maintains memories by regulating GluR2-dependent AMPA receptor trafficking.** *Nat Neurosci* 2010:in press. doi:10.1038/nn.2531.
  6. Muslimov IA, Nimmrich V, Hernandez AI, Tcherepanov A, Sacktor TC, Tiedge H: **Dendritic transport and localization of protein kinase M $\zeta$  mRNA: implications for molecular memory consolidation.** *J Biol Chem* 2004, **279**:52613-52622.
  7. Osten P, Valsamis L, Harris A, Sacktor TC: **Protein synthesis-dependent formation of protein kinase M $\zeta$  in long-term potentiation.** *J Neurosci* 1996, **16**:2444-2451.
  8. Puls A, Schmidt S, Grawe F, Stabel S: **Interaction of protein kinase C  $\zeta$  with ZIP, a novel protein kinase C-binding protein.** *Proc Natl Acad Sci U S A* 1997, **94**:6191-6196.
  9. Serrano P, Yao Y, Sacktor TC: **Persistent phosphorylation by protein kinase M $\zeta$  maintains late-phase long-term potentiation.** *J Neurosci* 2005, **25**:1979-1984.
  10. Serrano P, Friedman EL, Kenney J, Taubenfeld SM, Zimmerman JM, Hanna J, Alberini C, Kelley AE, Maren S, Rudy JW, et al: **PKM $\zeta$  maintains spatial, instrumental, and classically conditioned long-term memories.** *PLoS Biol* 2008, **6**:e318.
  11. Shema R, Sacktor TC, Dudai Y: **Rapid Erasure of Long-Term Memory Associations in the Cortex by an Inhibitor of PKM $\zeta$ .** *Science* 2007, **317**:951-953.
  12. Kelly MT, Crary JF, Sacktor TC: **Regulation of protein kinase M $\zeta$  synthesis by multiple kinases in long-term potentiation.** *J*

- Neurosci* 2007, **27**:3439-3444.
13. Ogasawara H, Doi T, Kawato M: **Systems biology perspectives on cerebellar long-term depression.** *NeuroSignals* 2008, **16**:300-317.
  14. Bhalla US, Iyengar R: **Emergent properties of networks of biological signaling pathways.** *Science* 1999, **283**:381-387.
  15. Ferrell JE, Jr.: **Building a cellular switch: more lessons from a good egg.** *Bioessays* 1999, **21**:866-870.
  16. Crick F: **Memory and molecular turnover.** *Nature* 1984, **312**:101.
  17. Lisman JE: **A mechanism for memory storage insensitive to molecular turnover: a bistable autophosphorylating kinase.** *Proc Natl Acad Sci U S A* 1985, **82**:3055-3057.
  18. Ogasawara H, Kawato M: **Computational models of cerebellar long-term memory.** In *Systems Biology: The Challenge of Complexity*. Edited by Nakanishi S, Kageyama R, Watanabe D. New York: Springer; 2009: 169-182
  19. Gamble E, Koch C: **The dynamics of free calcium in dendritic spines in response to repetitive synaptic input.** *Science* 1987, **236**:1311-1315.
  20. Chetkovich DM, Gray R, Johnston D, Sweatt JD: **N-methyl-D-aspartate receptor activation increases cAMP levels and voltage-gated Ca<sup>2+</sup> channel activity in area CA1 of hippocampus.** *Proc Natl Acad Sci U S A* 1991, **88**:6467-6471.
  21. Yuste R, Majewska A, Cash SS, Denk W: **Mechanisms of calcium influx into hippocampal spines: heterogeneity among spines, coincidence detection by NMDA receptors, and optical quantal analysis.** *J Neurosci* 1999, **19**:1976-1987.
  22. Rae MG, Martin DJ, Collingridge GL, Irving AJ: **Role of Ca<sup>2+</sup> stores in metabotropic L-glutamate receptor-mediated supralinear Ca<sup>2+</sup> signaling in rat hippocampal neurons.** *J Neurosci* 2000, **20**:8628-8636.
  23. Xia Z, Storm DR: **The role of calmodulin as a signal integrator for synaptic plasticity.** *Nat Rev Neurosci* 2005, **6**:267-276.

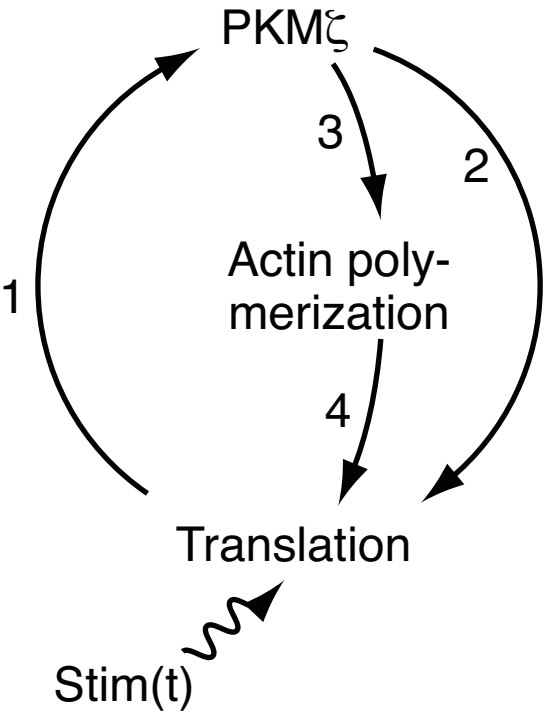
24. Lisman J, Spruston N: **Postsynaptic depolarization requirements for LTP and LTD: a critique of spike timing-dependent plasticity.** *Nat Neurosci* 2005, **8**:839-841.
25. Ling DS, Benardo LS, Serrano PA, Blace N, Kelly MT, Crary JF, Sacktor TC: **Protein kinase M $\zeta$  is necessary and sufficient for LTP maintenance.** *Nat Neurosci* 2002, **5**:295-296.
26. Gómez J, Martínez de Aragón A, Bonay P, Pitton C, García A, Silva A, Fresno M, Alvarez F, Rebollo A: **Physical association and functional relationship between protein kinase C  $\zeta$  and the actin cytoskeleton.** *Eur J Immunol* 1995, **25**:2673-2678.
27. Wang HR, Zhang Y, Ozdamar B, Ogunjimi AA, Alexandrova E, Thomsen GH, Wrana JL: **Regulation of cell polarity and protrusion formation by targeting RhoA for degradation.** *Science* 2003, **302**:1775-1779.
28. Chodniewicz D, Zhelev DV: **Chemoattractant receptor-stimulated F-actin polymerization in the human neutrophil is signaled by 2 distinct pathways.** *Blood* 2003, **101**:1181-1184.
29. Sun R, Gao P, Chen L, Ma D, Wang J, Oppenheim JJ, Zhang N: **Protein kinase C  $\zeta$  is required for epidermal growth factor-induced chemotaxis of human breast cancer cells.** *Cancer Res* 2005, **65**:1433-1441.
30. Stapulionis R, Kolli S, Deutscher MP: **Efficient mammalian protein synthesis requires an intact F-actin system.** *J Biol Chem* 1997, **272**:24980-24986.
31. Kelly MT, Yao Y, Sondhi R, Sacktor TC: **Actin polymerization regulates the synthesis of PKM $\zeta$  in LTP.** *Neuropharmacology* 2007, **52**:41-45.
32. Ermentrout B: *Simulating, Analyzing, and Animating Dynamical Systems: A Guide to XPPAUT for Researchers and Students.* 1st edn: Society for Industrial Mathematics; 2002.
33. Fall CP, Marland ES, Wagner JM, Tyson JJ: *Computational Cell Biology.* New York: Springer-Verlag; 2002.

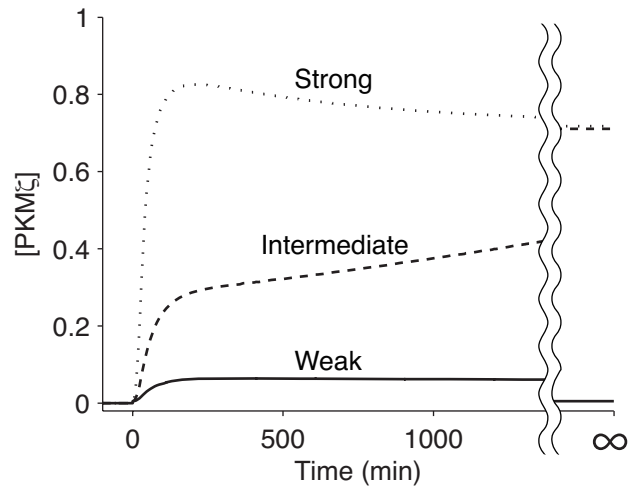
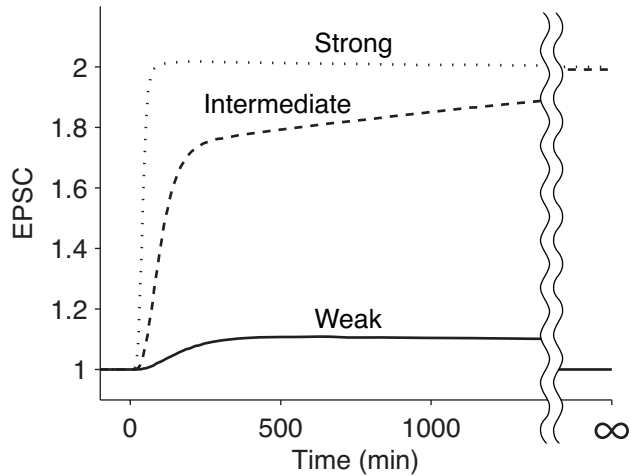
34. Kuznetsov YA: *Elements of applied bifurcation theory*. 3rd edn. New York: Springer; 2004.
35. Sara SJ: **Retrieval and reconsolidation: toward a neurobiology of remembering.** *Learn Mem* 2000, **7**:73-84.
36. Tronson NC, Taylor JR: **Molecular mechanisms of memory reconsolidation.** *Nat Rev Neurosci* 2007, **8**:262-275.
37. Nader K, Hardt O: **A single standard for memory: the case for reconsolidation.** *Nat Rev Neurosci* 2009, **10**:224-234.
38. Wanisch K, Wotjak CT: **Time course and efficiency of protein synthesis inhibition following intracerebral and systemic anisomycin treatment.** *Neurobiol Learn Mem* 2008, **90**:485-494.
39. Krucker T, Siggins GR, Halpain S: **Dynamic actin filaments are required for stable long-term potentiation (LTP) in area CA1 of the hippocampus.** *Proc Natl Acad Sci U S A* 2000, **97**:6856-6861.
40. Debiec J, LeDoux JE, Nader K: **Cellular and systems reconsolidation in the hippocampus.** *Neuron* 2002, **36**:527-538.
41. Fonseca R, Nagerl UV, Bonhoeffer T: **Neuronal activity determines the protein synthesis dependence of long-term potentiation.** *Nat Neurosci* 2006, **9**:478-480.
42. Arshavsky YI: **Long-term memory: does it have a structural or chemical basis?** *Trends Neurosci* 2003, **26**:465-466; author reply 466-468.
43. Whitlock JR, Heynen AJ, Shuler MG, Bear MF: **Learning induces long-term potentiation in the hippocampus.** *Science* 2006, **313**:1093-1097.
44. Wehland J, Osborn M, Weber K: **Phalloidin-induced actin polymerization in the cytoplasm of cultured cells interferes with cell locomotion and growth.** *Proc Natl Acad Sci U S A* 1977, **74**:5613-5617.
45. Hommel JD, Sears RM, Georgescu D, Simmons DL, DiLeone RJ: **Local gene knockdown in the brain using viral-mediated RNA interference.** *Nat Med* 2003, **9**:1539-1544.

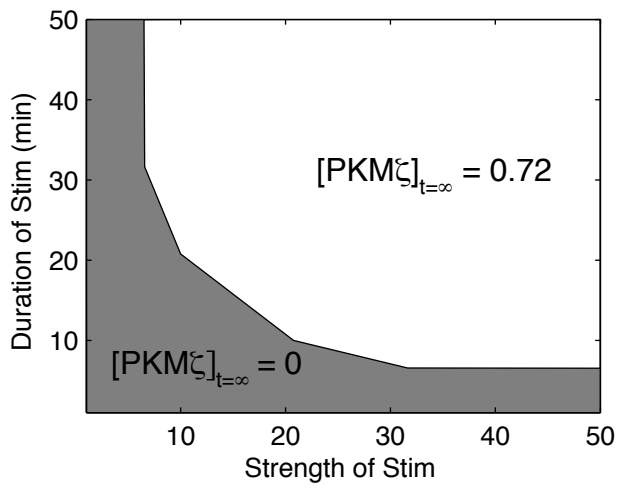
46. Le Gal La Salle G, Robert JJ, Berrard S, Ridoux V, Stratford-Perricaudet LD, Perricaudet M, Mallet J: **An adenovirus vector for gene transfer into neurons and glia in the brain.** *Science* 1993, **259**:988-990.
47. Ferrell JE, Jr., Machleder EM: **The biochemical basis of an all-or-none cell fate switch in *Xenopus* oocytes.** *Science* 1998, **280**:895-898.
48. Kuroda S, Schweighofer N, Kawato M: **Exploration of signal transduction pathways in cerebellar long-term depression by kinetic simulation.** *J Neurosci* 2001, **21**:5693-5702.
49. Huang CY, Ferrell JE, Jr.: **Ultrasensitivity in the mitogen-activated protein kinase cascade.** *Proc Natl Acad Sci U S A* 1996, **93**:10078-10083.
50. Miller P, Zhabotinsky AM, Lisman JE, Wang XJ: **The stability of a stochastic CaMKII switch: dependence on the number of enzyme molecules and protein turnover.** *PLoS Biol* 2005, **3**:e107.
51. Aslam N, Kubota Y, Wells D, Shouval HZ: **Translational switch for long-term maintenance of synaptic plasticity.** *Mol Syst Biol* 2009, **5**:284.
52. Ito M: **Cerebellar long-term depression: characterization, signal transduction, and functional roles.** *Physiol Rev* 2001, **81**:1143-1195.
53. Malenka RC, Bear MF: **LTP and LTD: an embarrassment of riches.** *Neuron* 2004, **44**:5-21.
54. Lynch MA: **Long-term potentiation and memory.** *Physiol Rev* 2004, **84**:87-136.
55. Hansel C: **When the B-team runs plasticity: GluR2 receptor trafficking in cerebellar long-term potentiation.** *Proc Natl Acad Sci U S A* 2005, **102**:18245-18246.
56. Hansel C, de Jeu M, Belmeguenai A, Houtman SH, Buitendijk GH, Andreev D, De Zeeuw CI, Elgersma Y:  **$\alpha$ CaMKII is essential for cerebellar LTD and motor learning.** *Neuron* 2006, **51**:835-843.

57. Kotaleski JH, Lester D, Blackwell KT: **Subcellular interactions between parallel fibre and climbing fibre signals in Purkinje cells predict sensitivity of classical conditioning to interstimulus interval.** *Integr Physiol Behav Sci* 2002, **37**:265-292.
58. Doi T, Kuroda S, Michikawa T, Kawato M: **Inositol 1,4,5-trisphosphate-dependent Ca<sup>2+</sup> threshold dynamics detect spike timing in cerebellar Purkinje cells.** *J Neurosci* 2005, **25**:950-961.
59. Tanaka K, Khiroug L, Santamaria F, Doi T, Ogasawara H, Ellis-Davies GC, Kawato M, Augustine GJ: **Ca<sup>2+</sup> requirements for cerebellar long-term synaptic depression: role for a postsynaptic leaky integrator.** *Neuron* 2007, **54**:787-800.
60. Tanaka K, Augustine GJ: **A positive feedback signal transduction loop determines timing of cerebellar long-term depression.** *Neuron* 2008, **59**:608-620.
61. Oster H, Eichele G, Leitges M: **Differential expression of atypical PKCs in the adult mouse brain.** *Brain Res Mol Brain Res* 2004, **127**:79-88.
62. Ogasawara H, Kawato M: **Bistable Switches for Synaptic Plasticity.** *Sci Signal* 2009, **2**:pe7-.
63. Kasai H, Matsuzaki M, Noguchi J, Yasumatsu N, Nakahara H: **Structure-stability-function relationships of dendritic spines.** *Trends Neurosci* 2003, **26**:360-368.
64. Segal M: **Dendritic spines and long-term plasticity.** *Nat Rev Neurosci* 2005, **6**:277-284.
65. Hernandez PJ, Abel T: **The role of protein synthesis in memory consolidation: progress amid decades of debate.** *Neurobiol Learn Mem* 2008, **89**:293-311.
66. Saneyoshi T, Fortin DA, Soderling TR: **Regulation of spine and synapse formation by activity-dependent intracellular signaling pathways.** *Curr Opin Neurobiol* 2009, **20**:1-8.
67. Xu T, Yu X, Perlik AJ, Tobin WF, Zweig JA, Tennant K, Jones T, Zuo Y:

- Rapid formation and selective stabilization of synapses for enduring motor memories.** *Nature* 2009, **462**:915-919.
68. Yang G, Pan F, Gan WB: **Stably maintained dendritic spines are associated with lifelong memories.** *Nature* 2009, **462**:920-924.
69. Jaworski J, Kapitein LC, Gouveia SM, Dortland BR, Wulf PS, Grigoriev I, Camera P, Spangler SA, Di Stefano P, Demmers J, et al: **Dynamic Microtubules Regulate Dendritic Spine Morphology and Synaptic Plasticity.** *Neuron* 2009, **61**:85-100.
70. Jain P, Bhalla US: **Signaling logic of activity-triggered dendritic protein synthesis: an mTOR gate but not a feedback switch.** *PLoS Comput Biol* 2009, **5**:e1000287.
71. Le Good JA, Brindley DN: **Molecular mechanisms regulating protein kinase C $\zeta$  turnover and cellular transformation.** *Biochem J* 2004, **378**:83-92.
72. Star EN, Kwiatkowski DJ, Murthy VN: **Rapid turnover of actin in dendritic spines and its regulation by activity.** *Nat Neurosci* 2002, **5**:239-246.
73. Tataavarty V, Kim EJ, Rodionov V, Yu J: **Investigating sub-spine actin dynamics in rat hippocampal neurons with super-resolution optical imaging.** *PLoS One* 2009, **4**:e7724.
74. Mayer ML: **Glutamate receptor ion channels.** *Curr Opin Neurobiol* 2005, **15**:282-288.
75. Greger IH, Ziff EB, Penn AC: **Molecular determinants of AMPA receptor subunit assembly.** *Trends Neurosci* 2007, **30**:407-416.
76. Zhao C, Slevin JT, Whiteheart SW: **Cellular functions of NSF: not just SNAPs and SNAREs.** *FEBS Lett* 2007, **581**:2140-2149.



**A****B**

**A****B**